Impact of impurities on energy confinement bifurcation at density above the Greenwald limit in DIII-D high-β_P plasmas

EXC

S. Ding[1*], S. Shi[2], A.M. Garofalo[1], B. Van Compernolle[1], D.B. Weisberg[1], H. Wang[1], D. Eldon[1], B.S. Victor[3], A. Marinoni[4], Q.M. Hu[5], I.S. Carvalho[1], L. Wang[6], A.W. Hyatt[1], T.H. Osborne[1], X.Z. Gong[6], J.P. Qian[6], J. Huang[6], C.T. Holcomb[3] and J.M. Hanson[7]

[1]General Atomics, PO Box 85608, San Diego, California 92186-5608, USA
[2]Oak Ridge Associated Universities, Oak Ridge, TN 37831, United States of America
[3]Lawrence Livermore National Laboratory, Livermore, California
[4]University of California San Diego, La Jolla, CA, 92093, USA
[5]Princeton Plasma Physics Laboratory, Princeton University, Princeton, NJ, 08543, USA
[6]Institute of Plasma Physics, Chinese Academy of Sciences, PO Box 1126, Hefei, Anhui 230031, China
[7]Department of Applied Mathematics and Applied Physics, Columbia University, New York, New York 10027-6900, USA

[*]Email: dingsiye@fusion.gat.com

A bifurcation of global confinement, which is associated with core impurity levels, has been observed in DIII-D high poloidal-beta (β_P) experiments, enabling further improved energy confinement at line-averaged density above the Greenwald limit ($f_{Gr}=\bar{n}_e/n_{Gr}>1$). It can be recognized as a third bifurcation in the high-β_P plasmas after the first bifurcation which triggers the transition to H-mode and the second one which forms large-radius internal transport barrier (ITB). Both DIII-D database (non-high-β_P and high-β_P) and the ITPA international database suggest decreased maximum H_{98y2} at increased density in experiment. At IAEA FEC 2023, we reported the first-time achievement in tokamak H-mode experiments --- the development of DIII-D high-β_P scenario with simultaneous density above the Greenwald limit (f_{Gr} up to 1.25) and H_{98y2}~1.5 [1, 2]. Most recent high-β_P experiment on DIII-D has another breakthrough, achieving f_{Gr}~1.45 and H_{98y2}~1.4 at even slightly higher plasma current. Although the exciting experimental results extend the operating boundary towards an uncharted regime, detailed analysis reveals the existence of secondary global confinement bifurcations in these plasmas, indicating the impurity effect on limiting energy confinement quality at high density. This synopsis reports a relatively higher confinement state and a relatively lower confinement state at the same density above the Greenwald limit in some high-β_P discharges. Lower confinement relates to higher core radiated power induced by intrinsic high-Z impurities on DIII-D.

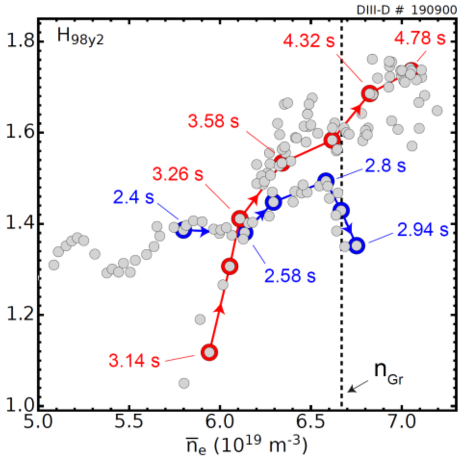

Fig. 1 Grey dots: H_{98y2} and $\bar{n}_e$ at different time slices in DIII-D #190900. A smoothing window of 50 ms is applied to H_{98y2}.

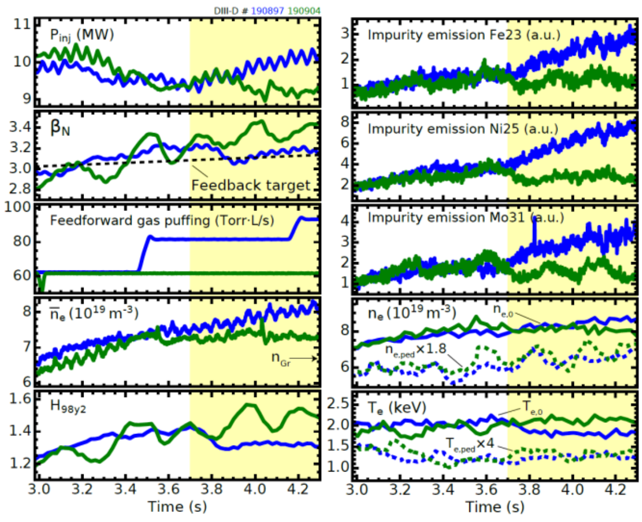

Fig. 2 Time histories of DIII-D #190897 (blue) and #190904 (green). Shaded area indicates the period that reduced energy confinement happens along with higher high-Z impurity emission.

Fig. 1 shows an example of energy confinement bifurcation and the lower confinement branch shows a rollover in the plot of H_{98y2} vs $\bar{n}_e$, indicating reduced H_{98y2} at higher density, while the higher confinement branch suggests higher H_{98y2} with no rollover observed. The equilibria at 2.58 s and at 3.26 s both have ITBs at the same large radius, resulting in close $\bar{n}_e$ and similar H_{98y2}. However, divergence is observed at higher density. The transition from the lower confinement branch to the higher one happens at 2.99 s in DIII-D #190900, due to a minor β-collapse. H_{98y2} in the lower confinement branch evolves to <1.4 later at higher density, while that of in the higher confinement branch reaches >1.7.

Fig. 2 shows another example when comparing two similar high-β_P discharges at density above the Greenwald limit. These two discharges have the same I_p and B_T, and they have very similar plasma performance at the same D_2 gas puffing rate before 3.5 s. The experiment aims at pursuing higher density at higher level of active gas puffing. When higher feedforward D_2 gas puffing rate is applied on #190897 (blue), higher line-averaged density is achieved successfully. But reduced H_{98y2} and $T_{e,0}$ are also observed together with various increased high-Z impurity line-emission (e.g. Fe^{23+}, Ni^{25+} and Mo^{31+}) from 3.7 s (shaded area in fig. 2). Note that although the PFC material of main chamber and divertors of DIII-D is carbon, there are some intrinsic high-Z metallic impurities from Inconel vacuum vessel and RF antenna straps. The increased high-Z impurities cause higher radiated power in the plasma core, which leads to decreasing plasma performance (β_N) and energy confinement (H_{98y2}) until compensation from increased injected power. Although the discharge is under β_N feedback control, the control system does not respond to the decrease of β_N immediately, e.g. 3.7 s - 3.85 s. This is because the β_N is above the feedback target when the confinement starts to drop. With additional 0.7 MW NBI power later on, β_N is sustained at the feedback target, and H_{98y2} is also maintained, however, at a level lower than the previous achieved value at 3.7 s. The H_{98y2} is also lower than that of the discharge (green in fig. 2) without increased gas puffing and increased impurity emissions. As shown in fig. 2, the pedestal density and temperature are almost identical in these two discharges after 3.7 s, when the divergence of energy confinement emerges. This confirms that the change in the core is responsible for the reduced confinement. MHD behaviors for n=1, 2, 3 are also almost identical.

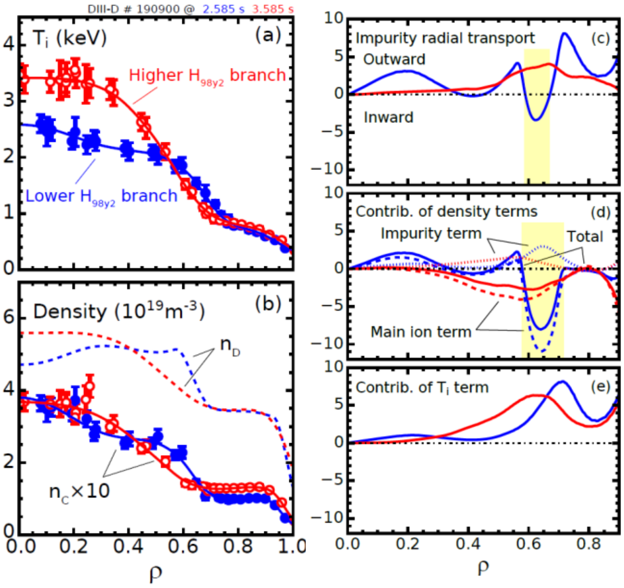

Fig. 3 Profiles of DIII-D #190900 at 2.585 s (blue) and 3.585 s (red). Shaded area indicates impurity pinch predicted by neoclassical theory for the 2.585 s case.

Studying the different confinement branches could lead to better understanding of how to maximize H_{98y2} at high density. Detailed profile analysis suggests that lower H_{98y2} branch is associated with too high density gradient along or not high enough temperature gradient. Fig. 3 shows one example from the discharges in fig. 1. The lower H_{98y2} case has strong main ion density gradient at ρ~0.6-0.7 (fig. 3(b)), which results in strong impurity pinch effect (fig. 3(d)) according to neoclassical theory, radial transport $R\langle\Gamma_Z^{neo}\rangle \propto \frac{1}{Z}\frac{R}{L_{nz}} - \frac{R}{L_{ni}} + \frac{1}{2}\frac{R}{L_{Ti}}$ [3], where L_n and L_T are scale lengths of density and temperature (e.g. $L_n=n/\nabla n$), respectively. High gradient in T_i profile indeed offsets the neoclassical impurity radial transport outwards. The impurity inward transport region becomes smaller when taking the contribution of T_i term into account, i.e. comparing the shaded area in fig. 3(c) and 3(d). Unfortunately, the T_i gradient in the lower H_{98y2} case decreases inside ρ~0.65, leaving net impurity pinch around ρ~0.6. On the other hand, the higher H_{98y2} case has weaker impurity pinch effect from L_{ni} term, and has stronger outward transport contribution from L_{Ti} term. It leads to a feature of net outward impurity neoclassical radial transport from magnetic axis to pedestal. The analysis is qualitatively consistent with the experimental observations of lower impurity core radiation in the higher H_{98y2} cases.

In conclusion, the preliminary analysis suggests that the level of core radiation induced by impurity accumulation is responsible for the observed energy confinement bifurcation in the high-β_P plasmas at density around the Greenwald limit. Further analysis of the turbulent impurity transport will be considered in the next step. The existence of higher energy confinement branch indicates that there could be a balance between density gradient and temperature gradient for optimized impurity transport. Knowing the governing physics, potential experimental approaches to further control impurity accumulations in the high-β_P plasmas can be developed and lead to improved energy confinement quality at line-averaged density above the Greenwald limit.

Acknowledgements

This work was supported in part by the US Department of Energy under DE-FC02-04ER54698 and DE-SC0010685, DE-AC52-07NA27344, DE-FG02-04ER54761, DE-AC02-09CH11466 and DE-SC0016154).

Reference

[1] S. Ding *et al.*, 29th IAEA FEC **EX/P2-7**, Oct. 16-21, 2016, London, UK
[2] S. Ding *et al.*, *Nature* **629** (2024) 555
[3] C. Angioni, *Plasma Phys. Control. Fusion* **63** (2021) 073001